Unusual excimer/dimer behaviour of a highly soluble C,N platinum(II) complex with a spiro-fluorene motif

Piotr Pander,[a],[b]* Andrey V. Zaytsev,[c] Larissa Gomes Franca,[d],[e] Fernando B. Dias[d]* and Valery N. Kozhevnikov[c]*

[a] *Faculty of Chemistry, Silesian University of Technology, Strzody 9, 44-100 Gliwice, Poland. E-mail: piotr.pander@polsl.pl*
[b] *Centre for Organic and Nanohybrid Electronics, Silesian University of Technology, Konarskiego 22B, 44-100 Gliwice, Poland*
[c] *Department of Applied Sciences, Faculty of Health and Life Sciences, Northumbria University, Newcastle Upon Tyne, Tyne and Wear, NE1 8ST, UK*
E-mail: valery.kozhevnikov@northumbria.ac.uk
[d] *Department of Physics, Durham University, Durham, South Road, DH1 3LE, UK*
E-mail: f.m.b.dias@durham.ac.uk
[e] *Department of Materials Science and Metallurgy, University of Cambridge, Cambridge CB3 0FS, UK*

Abstract

In this work we introduce a spiro-fluorene unit into a phenylpyridine (*CN*) type ligand as a simple way to de-planarise the structure and increase solubility of the final platinum(II) complex. Using a spirofluorene unit, orthogonal to the main coordination plane of the complex, reduces intermolecular interactions, leading to increased solubility but without significantly affecting complex ability to form Pt···Pt dimers and excimers. This approach is highly important in the design of platinum(II) complexes, which often suffer from low solubility due to their mainly planar structure, and offers an alternative to the use of bulky alkyl groups. The non-planar structure is also beneficial for vacuum-deposition techniques as it lowers the sublimation temperature. Importantly, there are no sp^3 hybridised carbon atoms in the cyclometallating ligand that contain hydrogens, the undesired feature that is associated with the low stability of the materials in OLEDs. The complex displays high solubility in toluene ~10 mg mL^{-1} at room temperature, which allows producing solution-processed OLEDs in a wide range of doping concentrations, 5-100% and EQE up to 5.9% with a maximum luminance of 7 400 cd m^{-2}. Concurrently, we have also produced vacuum-deposited OLEDs, which display luminance up to 32 500 cd m^{-2} and maximum EQE of 11.8 %.

Introduction

Low solubility or high susceptibility to aggregation is a common feature of planar luminophores, such as platinum(II) complexes[1–3] or multiple resonance TADF emitters (MR-TADF)[4] for example. This behaviour originates from relatively strong interplanar π···π interactions which in planar structures are completely undisturbed. If high solubility or low aggregation are desired, the typical way to tackle the problem is by decorating the structure of luminophores with linear or branched alkyls,[5,6] cycloalkene units[7,8] or through the use of aromatic rings orthogonal to the main luminophore plane, such as mesitylene[9] or diisopropylphenyl.[10] A possible disadvantage of this approach is the appearance of additional rotavibrational motions associated with these groups leading to a potential luminescence quenching due to the enhanced non-radiative decay. The use of a spiro-linked fluorene unit orthogonal to the main coordination plane of the platinum complex poses an interesting approach in which the rigid aromatic groups are fixed in position. This design features a relatively rigid spiro linkage through a quaternary sp^3 carbon atom that not only reduces the non-radiative decay, but also eliminates conformational disorder leading to a more favourable behaviour of the luminophore in solid films and OLEDs.[11,12]

The low solubility of platinum(II) complexes poses a significant limitation in synthesis, characterisation, as well as on their use as luminescent dopants in organic light-emitting diodes (OLEDs). This is because strong intermolecular interactions, originating from π···π and Pt···Pt contacts are likely to be affecting their electronic properties.[13–15] This issue may be of even greater importance for diplatinum(II) complexes, where the planar conjugated structure is extended. These complexes are of particular interest due to their strong near infrared (NIR) luminescence[16] or short decay lifetimes due to thermally activated delayed fluorescence (TADF).[17] Selected Pt(II) complexes display strong Pt···Pt aggregation leading to efficient near infrared (NIR) photo- and electroluminescence.[18] Therefore, effective strategies for increasing solubility of the said complexes are needed, but such that do not completely restrict Pt···Pt contacts required for their NIR luminescence in solid state.

Processing emissive materials from solution poses significant advantages in terms of their use in low-cost or large area applications. For example, many features of potential commercial applications can be produced with inkjet, roll-to-roll printing or slot dye coating.[19,20] In this case the emitter molecule must be highly soluble in solvents that would pose low environmental as well as health and safety hazards. For example, the use of popular chlorinated solvents, such as chloroform, chlorobenzene or dichlorobenzene must be avoided. Instead, halogen-free aromatic solvents, such as toluene or xylenes can be used – ideally these can also be replaced with an appropriate *green solvent*.

Typically, white light OLEDs or WOLEDs require two emitters, *i.e.* blue and yellow to obtain white electroluminescence.[21] This can be achieved by mixing the two or more luminophores in an emissive layer in a specific proportion or through the use of tandem and multilayer structures.[22,23] A rather more favourable possibility is the use a single dopant that may give rise to the two luminescent bands which combined together may result in white electroluminescence. Single-dopant WOLEDs are significantly simpler, eliminating multiple variables affecting the optimal design of multicomponent structures. In this respect, excimer-forming platinum(II) complexes are a profound example of a luminophore where the control of the emitter concentration allows for fine tuning of the EL colour between sky blue, white, and yellow-orange.[14]

Diketone **1** (**Scheme 1**) was previously used to derive pyrazine-type cyclometallating ligands.[24] Having the above factors in mind we decided to use **1** as a basis to construct ligand **4** featuring the spiro fluorene unit. To the best of our knowledge the pyridine-type ligand **4** has not

been previously reported. We therefore decided to prepare it and to investigate its coordinating behaviour and thus obtain platinum(II) complex **7**.

Synthesis

In our synthesis we used 1,2,4-triazine derivative **3** as a key intermediate. The 1,2,4-triazine methodology is a versatile tool that we and others previously used to access various polypyridine-type ligands.[7] The diketone **1** was reacted with generated in-situ formamidrazone **2** to give 1,2,4-triazine **3** in 34% yield. 1,2,4-Triazines are well-known electron-deficient dienes that participate in inverse electron demand Diels-Alder reaction with electron-rich dienophiles. To prepare unsubstituted pyridine, the triazine **3** was reacted with excess of 2,5-norbornadiene to give the desired cyclometallating ligand **4** in 65% yield. The reaction required high temperature of 185°C. To avoid high-boiling point solvents, which are difficult to remove, the reaction was carried out in toluene in a sealed pressure tube. It should be noted that the 1,2,4-triazine method allows functionalisation of the pyridine ring by using a variety of electron-rich dienophiles providing a tool for further tuning of physical and emissive properties of the complexes. The ligand **3** was then used to prepare the target complex **7** in a well-known three step procedure. First, the ligand was heated under reflux in acetic acid with potassium tetrachloroplatinate to give the dichloro-bridged intermediate **5** which was then cleaved by heating with DMSO to give the DMSO complex **6**, which upon reacting with sodium acetylacetonate in refluxing acetone gave the desired product **7**. The overall yield from **3** to **7** was 17%.

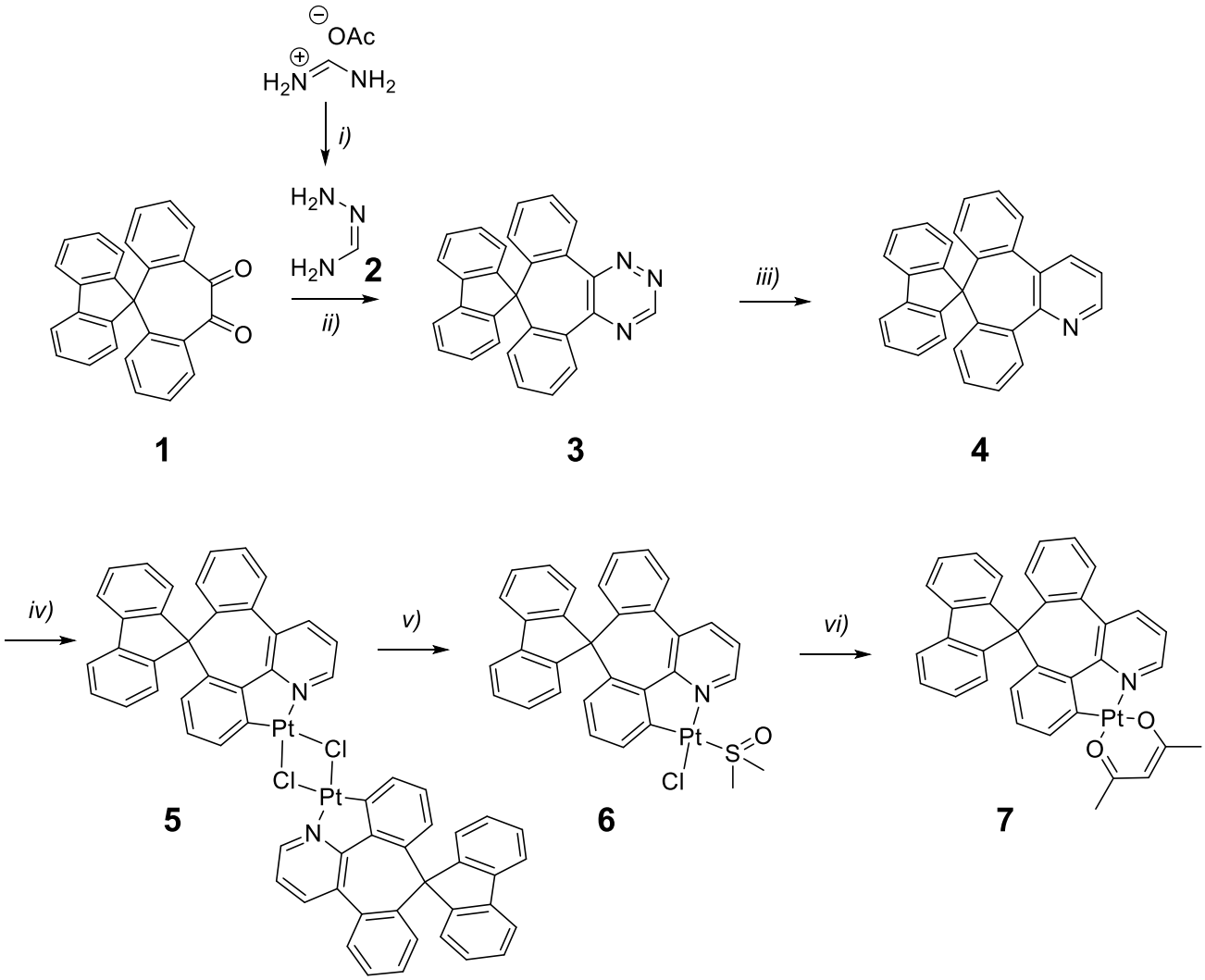

Scheme 1. Synthesis of the cyclometallating ligand **4** and its Pt(II) complex **7**. Reaction conditions: i) hydrazine hydrate, RT, MeOH, 2 min, *in-situ*; ii) 1,4-dioxane/DMF, RT, 24 hours, 34%; iii) 2,5-norbornadiene, toluene, sealed reactor, 185°C, 20h, 65%; iv) K_2PtCl_4, AcOH, reflux, 24 hours; v) DMSO, 130°C, 30 min; vi) Na(acac), acetone, reflux, 72 hours, 17% (overall for steps iv-vi).

Photophysics

Solution state

Absorption spectrum (**Figure 1**) of **7** in CH_2Cl_2 is rather typical of other platinum(II) complexes, with notable maxima at λ_{abs} = 260 nm (ε = 31300 M^{-1} cm^{-1}), λ_{abs} = 345 nm (ε = 10100 M^{-1} cm^{-1}), and an absorption shoulder at λ_{abs} ~405 nm (ε ~4200 M^{-1} cm^{-1}). Furthermore, we also observe an extremely weak absorption band at λ_{abs} = 493 nm (ε = 40 M^{-1} cm^{-1}), attributed to a spin-forbidden $S_0 \rightarrow T_1$ transition based on its overlap with the onset of the phosphorescence spectrum. Using the Strickler and Berg method[25] we estimate the radiative rate of the $T_1 \rightarrow S_0$ transition, which is comparable to that obtained directly (listed below), $k_r = 3 \times 10^4$ s^{-1}. This further confirms our attribution of the λ_{abs} = 493 nm band to a $S_0 \rightarrow T_1$ transition. Complex **7** displays a vibronically resolved PL spectrum at RT (λ_{PL} = 514 nm), with the vibronic structure even more evident at 77

K in 2MeTHF glass, with the (0,0) transition at 504 nm and extending out to 640 nm with a progression of ~1400 cm^{-1} (~170 meV). The complex is readily soluble in a variety of solvents and may be brought to a very high concentration. We study the complex in CH_2Cl_2 in the concentration range from 10^{-6} M to 10^{-3} M (**Figure 2**) which reveals a fair to low propensity (quenching constant 1.5×10^8 M^{-1} s^{-1}, ~30× lower than that reported for the archetypal excimer-forming Pt(bpyb)Cl[26]) to form low energy excited states typically assigned to excimers. This behaviour is fully in line with that of other platinum(II) complexes.[3,27–29] These findings indicate that the introduction of the spiro-linked fluorene significantly reduces the effective intermolecular interactions that lead to aggregation or excimer formation in solution. The newly formed excimer displays a broadband PL with λ_{PL} = 682 nm (**Figure S15**). The overall contribution of excimer PL is very low, even at 10^{-3} M, and therefore the decay traces recorded at λ_{col} = 515 nm and at λ_{col} = 750 nm appear nearly identical. However, the decay at λ_{col} = 750 nm subtly lags behind the λ_{col} = 515 nm, which is a feature usually observed for excimer formation in platinum(II) complexes in solution (**Figures S13** and **S14**). This is an expected behaviour which we discussed in our earlier works.[26,30] To further confirm the observed long wavelength PL band originates from excimers and not from ground state aggregates we record an absorption spectrum of a highly concentrated solution, c = 10^{-3} M (**Figure S10**). The absorption spectrum in this case is identical to that recorded at c = 10^{-5} M, indicating no significant quantities of aggregates being present. Decay lifetime of **7** at RT in CH_2Cl_2 at c→0 is estimated at τ = 7.1 μs. The lifetime rises to τ = 10.6 μs in 2MeTHF glass at 77 K (c = 10^{-5} M). **7** displays a photoluminescence quantum yield in solution of Φ_{PL} = 0.41 and a triplet radiative rate of k_r = 6.0×10^4 s^{-1}, very similar to that obtained using the Strickler and Berg method (see above).

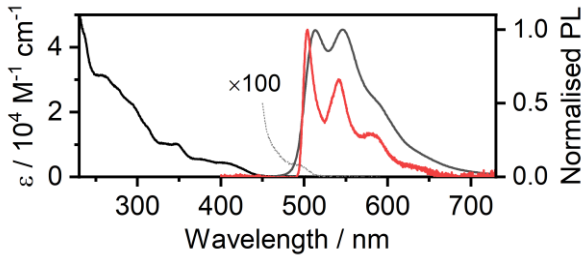

Figure 1. Absorption and PL spectrum (black and dark grey line, respectively) of **7** recorded in CH_2Cl_2 at RT as well as PL spectrum in 2MeTHF glass (red line) recorded at 77K (c = 10^{-5} M).

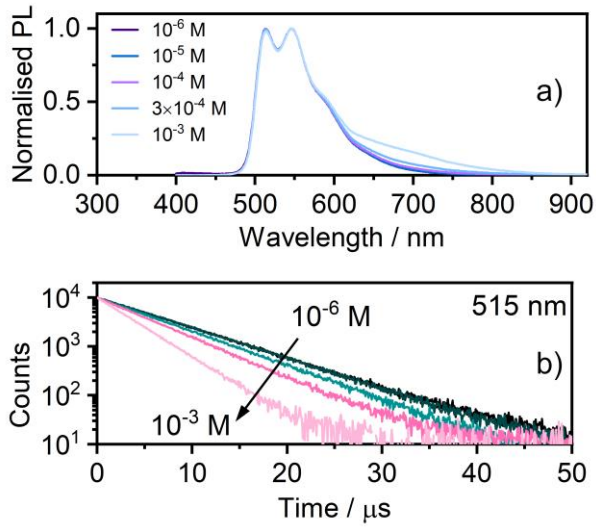

Figure 2. a) PL spectra in CH_2Cl_2 recorded at concentrations from 10^{-6} M to 10^{-3} M. b) PL decay traces recorded at λ_{col} = 515 nm for concentrations of **7** from 10^{-6} M to 10^{-3} M.

Solid state

We studied the behaviour of **7** in a model OLED host, a blend of PVK {poly(n-vinylcarbazole)} and PBD {2-(4-biphenyl)-5-(4-*tert*-butylphenyl)-1,3,4-oxadiazole} (**Figure 3**). **7** displays a similar behaviour in films to solution with a clearly resolved unimolecular PL, identical to that recorded in CH_2Cl_2. It also forms a broad and low energy PL band (λ_{PL} = 636 nm). We assign this emission to dimers based on our previous studies.[15,26] This assignment is in line with the behaviour of the PL spectra in film, where the intensity of the (0,0) component is reduced upon increased concentration due to a weak dimer absorption. Similar effect is not observed in a solution, where excimers dominate. Usually, excimers/dimers of a given Pt(II) complex are identical or at least very similar in solution and film due to the negligible effect of the environment on the bimolecular species' excited state energy. In fact, aggregate emission in film tends to be more red shifted due to the involvement of larger aggregates than dimers.[15,26] In the case of **7** we observe a more blue shifted PL in film in respect to solution (**Figure S15**). This unusual behaviour of the bimolecular emission suggests that solvent may be stabilising the excimer or that the solid state dimer is more rigid (and hence this is a rigidochromic effect). We explore the bimolecular excited state of **7** in the computational section below.

7 decays with an average lifetime (based on a biexponential fit) of τ_{av} = 13.0 μs and a Φ_{PL} = 0.39 in 5% loaded film – a similar lifetime is recorded in a frozen solution. This highlights the similarity between highly rigid solid phase at RT and a frozen solvent glass at 77 K. The decay lifetime of the 515 nm band shortens to only τ = 3.6 μs in 50% loaded film (Φ_{PL} = 0.30) and further to τ = 1.3 μs in the 100% film (Φ_{PL} = 0.14) for collection at 700 nm in the last case. An expected behaviour of the unimolecular (monomer) and the longer wavelength (aggregate) bands in platinum(II) complexes in films is such that the former always decays with a longer lifetime than the latter.[26,31] This is because the aggregate and monomer bands originate from distinct species existing in the ground state (*i.e.* aggregates formed from monomers) and decay naturally according to their respective radiative and non-radiative rates. In the case of **7** however we observe identical decay lifetime for collection at the 515 nm and 700 nm for the 15 and 50% loaded films. This suggest that the species are in fact in a form of an equilibrium where one species converts into another in a timescale much shorter than the luminescent decay. Given the

reduced molecular mobility in film in respect to solution it is unlikely for the luminophore to significantly migrate within the given timescale. In this case it is more likely for the molecules to oscillate around their centres of mass. We speculate that the behaviour of the monomer and aggregate bands originates from loosely bound dimers MM, which can oscillate between local excitation on one of the two units M+M* and a bimolecular excited state MM*. In other words, **7** appears to behave in film as if the molecule formed typical excimers rather than dimers. Given however the low mobility of molecules in solid films the most likely scenario is that they are already pre-organised into structures similar to dimers, yet they are loose enough to be able to form bimolecular excited states, but also, then, to dissociate into M + M* as it normally happens in a solution. This behaviour is highly unusual.

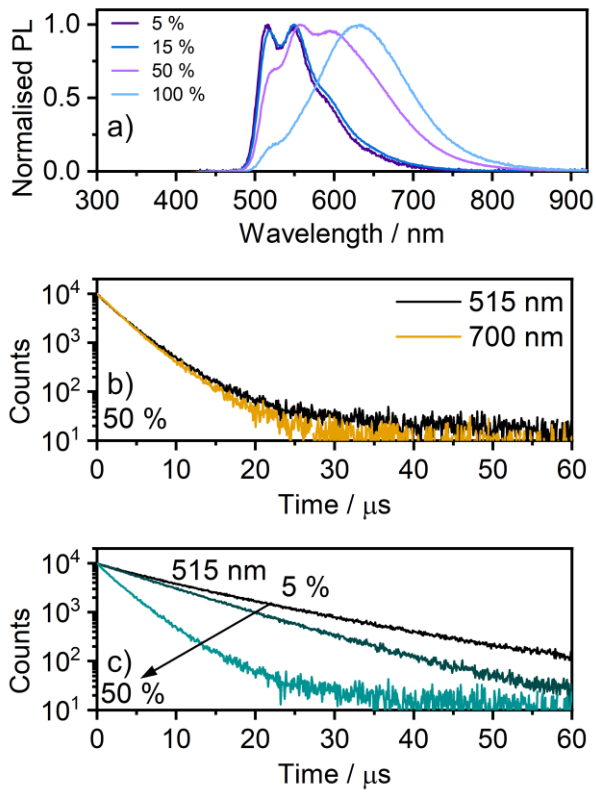

Figure 3. a) PL spectra in film of **7** doped into PVK:PBD blend (5-50%) and neat film. b) PL decay traces recorded at λ_{col} = 515 nm and λ_{col} = 700 nm. c) PL decay traces recorded at λ_{col} = 515 nm for concentrations of **7** in PVK:PBD film from 5 to 50%.

Calculations

We employ density functional theory (DFT) and time-dependent DFT (TD-DFT) using Orca[32] software to gain an in-depth understanding of the luminescent behaviour of the monomeric complex **7** and its bimolecular excited state. Ground state (S_0) and triplet excited state (T_1) geometries were optimised at the B3LYP[33,34]/def2-TZVP[35]/CPCM(CH_2Cl_2) level of theory. Phosphorescent radiative rates were obtained with the quasi-degenerate perturbation theory (QDPT)[36,37] using zeroth-order regular approximation (ZORA)[38,39] – corrected def2-TZVP basis sets[35] for light atoms and a segmented all-electron relativistically contracted (SARC) def2-TZVP basis set for Pt.

The molecule adapts a bent conformation of the *CN* ligand around the 7-membered ring with the spiro-linked fluorene unit, similar in S_0 and T_1. We note that experimental photoluminescence of **7**, λ_{PL} = 514 nm, is visibly red shifted in respect to that of related complexes, which display λ_{PL} < 500 nm,[13] especially in cases where the phenyl unit attached to the pyridine fragment is not connected to the *C*-coordinating part of the ligand and can rotate freely.[40] In the case of **7** the said phenyl unit is part planarized by the non-conjugating bridge to the *C*-coordinating fragment. We indeed observe that the non-coordinating third phenyl unit is to a small extent involved in HOMO and LUMO at the T_1-optimised geometry. However, otherwise its role is minimal and the λ_{PL} of **7** remains still relatively close to that of the related complexes with phenylpyridine chelating ligands. The fluorene unit is perpendicular to the *XY* plane set out by the *CN* ligand, but also displaced outwards of the structure along the *Z* axis. As a unit not conjugated with the rest of the *CN* ligand the fluorene moiety was not initially expected to take part in the lowest excited states. It does not contribute to the HOMO or LUMO, but it shows a clear contribution to the HOMO-1 and HOMO-2, likely due to its mild electron-donating capability.

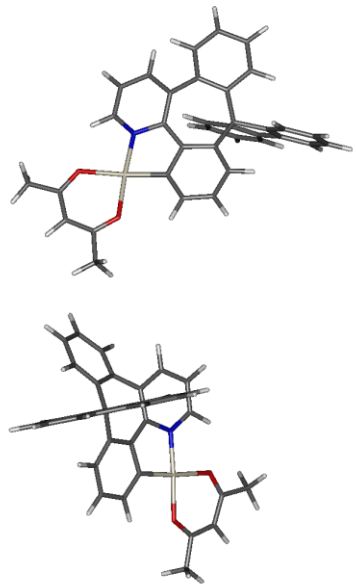

Figure 4. Optimised T_1 geometry of **7**.

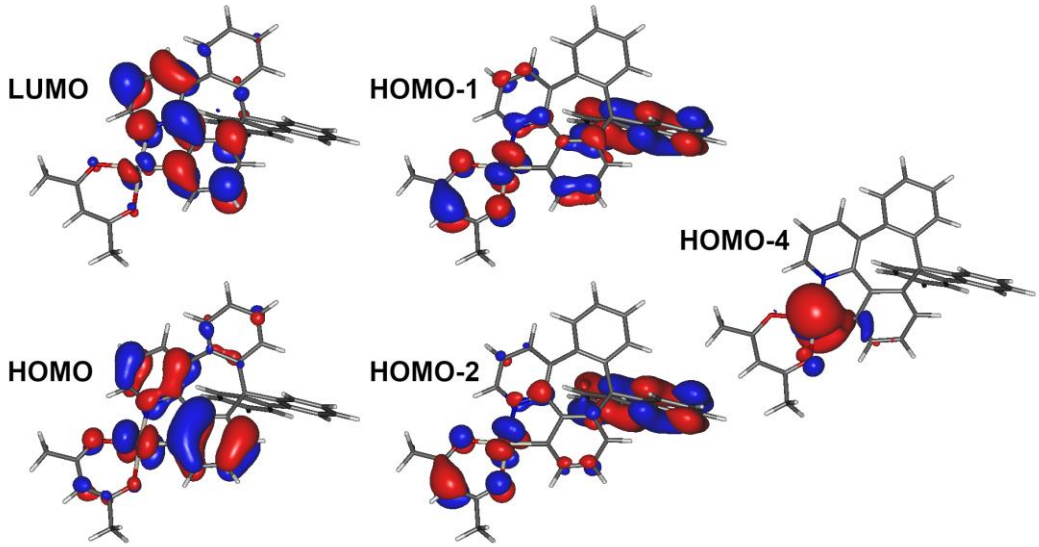

Figure 5. Iso surfaces of the molecular orbitals relevant to the T_1 and the S_1-S_4 excited states.

7 displays a small calculated zero-field splitting (ZFS), this is the energy difference between the split sublevels of the T_1 state, ZFS = 18.4 cm^{-1} and a calculated radiative rate of $k_r = 9\times10^4$ s^{-1}, in full agreement with the experimental result. The ZFS value is consistent with the mixed ^{3}LC (ligand centred) – ^{3}MLCT character of the emissive excited state.[41] The calculated energy of the $S_0 \rightarrow T_1$ transition, 2.71 eV (457 nm) is in-line with that recorded experimentally from the absorption spectrum. The phosphorescent properties of the complex originate from "borrowing" of the singlet radiative rate to the T_1.[42] For example, a modest S_1-T_1 spin-orbit coupling matrix element, SOCME = 23 cm^{-1}, is related to the similarity of the two states, both composed of >0.9 HOMO→LUMO excitation. Stronger coupling occurs for S_2-T_1, SOCME = 597 cm^{-1} and S_3-T_1, SOCME = 270 cm^{-1} pairs due to the involvement of a different *d* orbital of the metal centre in S_2 (HOMO-1→LUMO, 0.78) and S_3 (HOMO-2→LUMO, 0.80; HOMO-1→LUMO, 0.13). An even stronger coupling is displayed for the S_4-T_1 pair, SOCME = 1250 cm^{-1}, where the S_4 (HOMO-4→LUMO, 0.78) involves nearly exclusively the d_{z2} orbital of the metal centre.

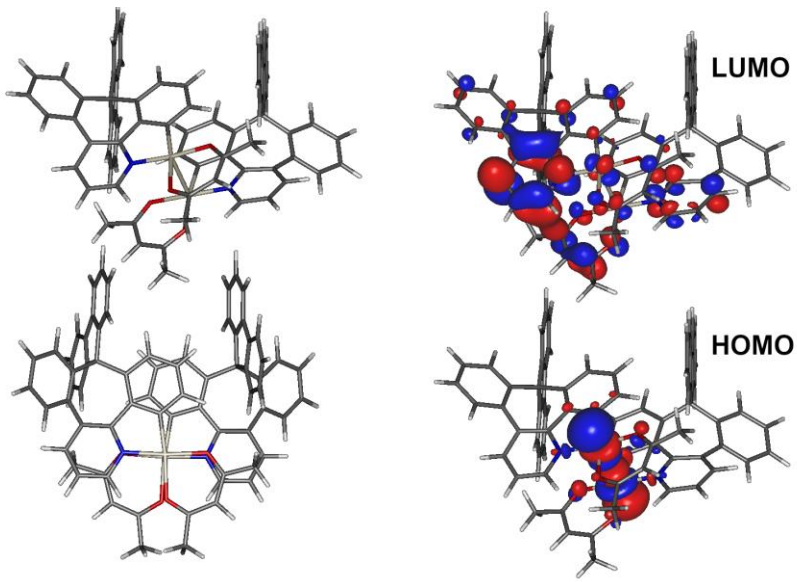

Figure 6. Excited state dimer of **7**: (*left*) A proposed optimised T_1 structure; (*right*) frontier molecular orbital iso surfaces.

In order to study the properties of the **7** excimer/dimer we constructed a model T_1 state dimer following the approach used successfully by us earlier.[15,26] The initial geometry comprised two molecules with a Pt···Pt distance of ~3 Å and with the bulky fluorene fragments facing outwards. The geometry was then optimised at the BP86/def2-svp level of theory, while the single point energy calculation at the optimised T_1 geometry was performed with B3LYP/def2-svp/CPCM(CH_2Cl_2). The structure of the excited state dimer presented in **Figure 6** displays the only minimal geometry obtained. For example, Pt(*NCN*)-X type complexes usually display two minima: head-to-tail and head-to-head structures with the former being the one most likely present in experimental systems.[26] In the case of **7** the two molecules are rotated one to another around the Pt···Pt axis by about 90° with all the other conformers prohibited due to the interaction between the fluorene unit and methyl groups of the acetylacetonate (acac) ancillary ligand. The dimer geometry displays a Pt···Pt distance of 2.82 Å and the fluorene units are pointing inwards of the structure. The coordination plane around the Pt centres is deformed from planarity with both the acac and phenylpyridine ligands tilted slightly outwards of the structure, but themselves remaining planar. The emissive triplet state, T_1 = 1.63 eV (760 nm) is of HOMO→LUMO nature. The HOMO is localised on the two metal centres with a clear contribution of their d_{z2} orbitals pointing towards each other, while the LUMO is distributed over the π-conjugated *CN* ligand, mostly on its pyridine fragment, forming a ^{3}MMLCT excited state.

Electroluminescence

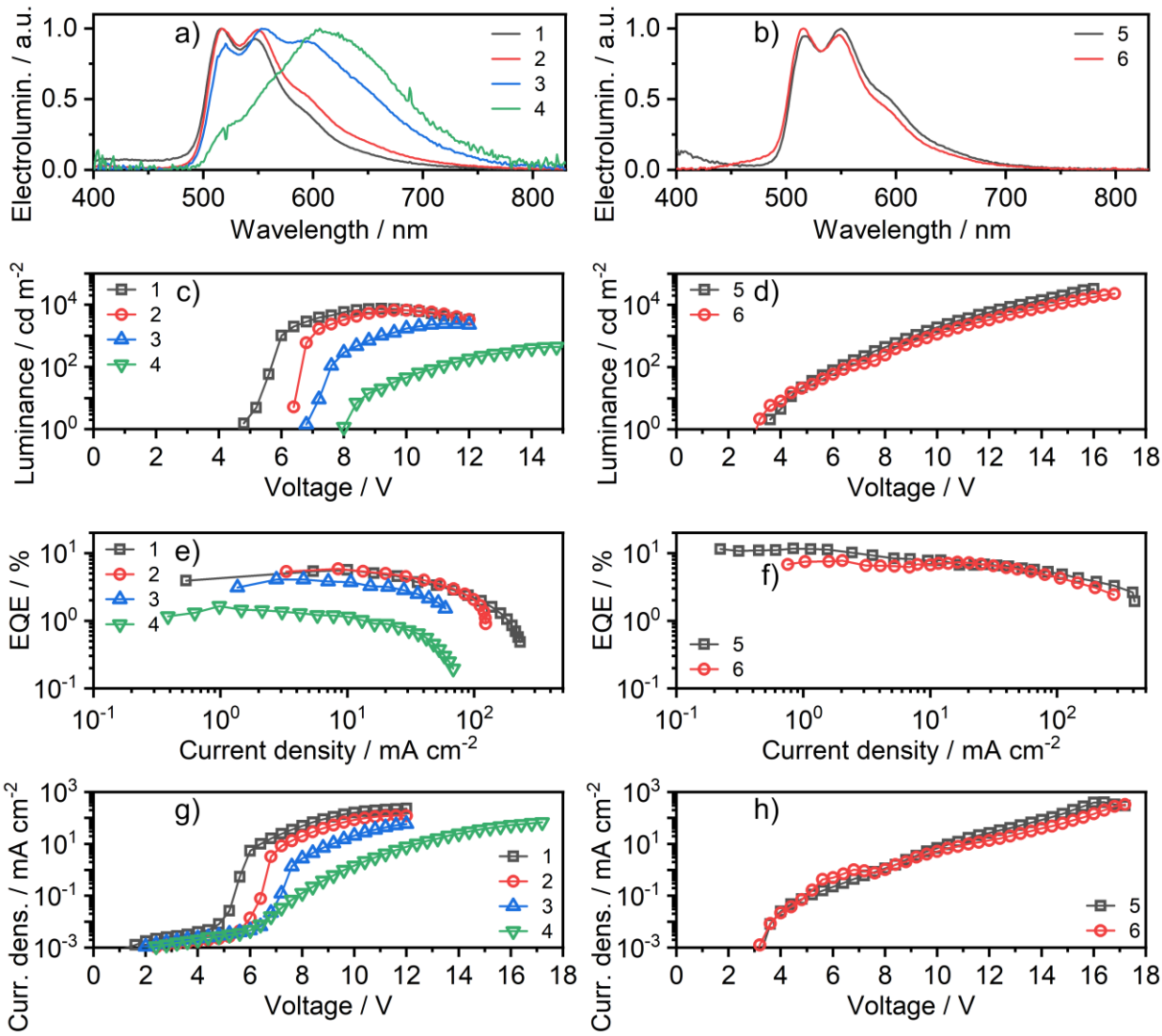

Figure 7. Characteristics of solution-processed OLED devices 1-4 and vacuum-deposited devices 5 and 6: *a)* and *b)* Electroluminescence spectra; *c)* and *d)* Luminance *vs* applied voltage; *e)* and *f)* External quantum efficiency (EQE) *vs* current density; *g)* and *h)* Current density *vs* applied voltage.

We produced prototype OLEDs to demonstrate the potential application of **7** in optoelectronic devices. Firstly, owing to the profound solubility of **7** in toluene we have produced solution-processed OLEDs 1-4 with a variable emitter load, from 5 to 100%, using a popular PVK:PBD host blend. Great solubility of the platinum(II) complex in toluene allows for the use of a more balanced structure involving a PVKH hole transport and electron blocking layer,[43] in comparison with structures where the emissive layer is placed directly on top of PEDOT:PSS. This structure allows for a relatively low turn-on voltage of ~5-7 V and luminance of up to 7400 cd m^{-2}. Progressively increasing the emitter load from 5% to 100% in the emissive layer results in a gradual increase in the contribution of the broadband and longer wavelength emission band, up to its dominance in the host-free OLED. The maximum external quantum efficiency (EQE) of the resultant OLEDs 1-4 follows the PLQY of the EML, with the maximum value of 5.9 % for the 15% loaded EML and the minimum value of 1.7 % for the non-doped device. A close comparison of

the PLQY and EQE values suggests that OLEDs 1-4 may not be fully optimised. Therefore, we fabricated fully vacuum-deposited OLEDs which can be easier optimised. Thus obtained OLEDs 5 and 6 display higher EQE of 11.8 and 7.5 %, respectively, and high luminance of up to 32500 cd m^{-2} with low turn-on voltage around ~3-3.5 V. The design of OLEDs 5 and 6 follows previous successful application of similar architectures to thermally activated delayed fluorescence (TADF) emitters.[44,45]

Although **7** does not display white electroluminescence due to the insufficiently blue shifted monomer PL, the behaviour of the complex highlights the possibility to use a similar molecular design in WOLEDs. In our case the small energy difference between the uni- and bimolecular emissions favours applications in WOLEDs as the lower energy band remains in its most in the visible region, reducing the contributions from the invisible near infrared tail. A further modification of the complex **7** could include decoration of the phenylpyridine fragment of the *CN* ligand with electron withdrawing groups to shift the monomer emission further to blue.[46]

Table 1. Characteristics of OLED devices 1-6.

	Dev 1	**Dev 2**	**Dev 3**	**Dev 4**	**Dev 5**	**Dev 6**
Emitter load, %	5	15	50	100	10	10
V_{ON} / V [a]	4.8	6.4	6.8	8.0	3.5	3.1
L_{max} / cd m^{-2} [b]	7400	6700	2300	400	32500	23300
λ_{EL} / nm [c]	517, 547, 590sh	517, 550, 594sh	519, 555, 595	522sh, 609	517, 550, 594sh	516, 548, 594sh
CIE 1931 (x, y) [d]	(0.34, 0.56)	(0.37, 0.58)	(0.45, 0.52)	(0.52, 0.46)	(0.36, 0.56)	(0.34, 0.58)
CE_{max} / cd A^{-1} [e]	19.8	19.9	10.5	3.8	38.9	25.5
EQE_{max} / % [f]	5.7	5.9	4.1	1.7	11.8	7.5

[a] turn-on voltage at 1 cd m^{-2}; [b] maximum luminance; [c] electroluminescence maxima; [d] colour coordinates of the electroluminescence spectrum as defined in the International Commission on Illumination colour space CIE 1931; [e] maximum current efficiency; [f] maximum external quantum efficiency.

Conclusion

1,2,4-Triazine methodology was used to access a novel cyclometallating ligand that contains a spiro-fluorene unit. The ability of the ligand to form cyclometallated complexes was proven by the synthesis of complex **7**. Other metal ions such as Ir(III) can potentially be used to provide access to a great variety of structures. The non-planar geometry of the ligand leads to high solubility of the complex in toluene and other solvents and effectively supresses the excimer formation in solution. However, in the solid state, the aggregation-type emission is observed for a 100% layer.

We observe an unusual behaviour of the excimer/dimer ^{3}MMLCT photoluminescence band formed by **7** at high concentration in film and in solution. Firstly, the long wavelength band is more red shifted in solution than film, while they should rather be identical, indicating that most likely the “rigid” environment of the solid film stabilises the excimer, while its stability is lower in solution (*i.e.* this is a rigidochromic effect). Secondly, the ^{3}MMLCT band displays similar kinetics

in film and solution, which is fundamentally surprising since the mechanisms underpinning formation of this PL band are different in the two media. We suggest that **7** displays an excimer-like behaviour in film, where the dimeric excited state MM* and the monomer – excited monomer pair M+M* are in an equilibrium, but without the associated relative displacement of the two units. This behaviour is unexpected since typically we observe the aggregate ^{3}MMLCT and the monomer ^{3}MLCT PL bands to decay independently, reflecting an aggregation-type scenario.

Finally, we use the novel complex **7** as the emitter in solution-processed and vacuum-deposited OLEDs. Thanks to the profound solubility of **7** in toluene we were able to obtain solution-processed emissive layers with 5-100% dopant content and a maximum luminance of 7 400 cd m^{-2} and ~6% EQE for the 5%-doped device. The fully vacuum-deposited OLEDs reached 32 500 cd m^{-2} and 11.8% EQE.

Supporting information

Supplementary ^{1}H and ^{13}C NMR spectra, experimental details, supplementary electrochemistry, photophysics, computational and OLED characterisation results (PDF).

References

(1) Li, K.; Ming Tong, G. S.; Wan, Q.; Cheng, G.; Tong, W.-Y.; Ang, W.-H.; Kwong, W.-L.; Che, C.-M. Highly Phosphorescent Platinum(II) Emitters: Photophysics, Materials and Biological Applications. *Chem. Sci.* **2016**, *7*, 1653–1673.

(2) Cocchi, M.; Kalinowski, J.; Virgili, D.; Williams, J. A. G. Excimer-Based Red/near-Infrared Organic Light-Emitting Diodes with Very High Quantum Efficiency. *Appl. Phys. Lett.* **2008**, *92*, 113302.

(3) Kim, D.; Brédas, J. L. Triplet Excimer Formation in Platinum-Based Phosphors: A Theoretical Study of the Roles of Pt-Pt Bimetallic Interactions and Interligand π-π Interactions. *J. Am. Chem. Soc.* **2009**, *131*, 11371–11380.

(4) Stavrou, K.; Danos, A.; Hama, T.; Hatakeyama, T.; Monkman, A. Hot Vibrational States in a High-Performance Multiple Resonance Emitter and the Effect of Excimer Quenching on Organic Light-Emitting Diodes. *ACS Appl. Mater. Interfaces* **2021**, *13*, 8643–8655.

(5) Ahn, D. H.; Kim, S. W.; Lee, H.; Ko, I. J.; Karthik, D.; Lee, J. Y.; Kwon, J. H. Highly Efficient Blue Thermally Activated Delayed Fluorescence Emitters Based on Symmetrical and Rigid Oxygen-Bridged Boron Acceptors. *Nat. Photonics* **2019**, *13*, 540–546.

(6) Lai, S.-L.; Tong, W.-Y.; Kui, S. C. F.; Chan, M.-Y.; Kwok, C.-C.; Che, C.-M. High Efficiency White Organic Light-Emitting Devices Incorporating Yellow Phosphorescent Platinum(II) Complex and Composite Blue Host. *Adv. Funct. Mater.* **2013**, *23*, 5168–5176.

(7) Pander, P.; Bulmer, R.; Martinscroft, R.; Thompson, S.; Lewis, F. W.; Penfold, T. J.; Dias, F. B.; Kozhevnikov, V. N. 1,2,4-Triazines in the Synthesis of Bipyridine Bisphenolate ONNO Ligands and Their Highly Luminescent Tetradentate Pt(II) Complexes for Solution-Processable OLEDs. *Inorg. Chem.* **2018**, *57*, 3825–3832.

(8) Kui, S. C. F.; Chow, P. K.; Cheng, G.; Kwok, C.-C.; Kwong, C. L.; Low, K.-H.; Che, C.-M. Robust Phosphorescent Platinum(Ii) Complexes with Tetradentate O∧N∧C∧N Ligands: High Efficiency OLEDs with Excellent Efficiency Stability. *Chem. Commun.* **2013**, *49*, 1497.

(9) Hall, D.; Suresh, S. M.; dos Santos, P. L.; Duda, E.; Bagnich, S.; Pershin, A.; Rajamalli, P.; Cordes, D. B.; Slawin, A. M. Z.; Beljonne, D.; Köhler, A.; Samuel, I. D. W.; Olivier, Y.; Zysman-Colman, E. Improving Processability and Efficiency of Resonant TADF Emitters:

A Design Strategy. *Adv. Opt. Mater.* **2020**, *8*, 1901627.

(10) Urban, M.; Marek-Urban, P. H.; Durka, K.; Luliński, S.; Pander, P.; Monkman, A. P. TADF Invariant of Host Polarity and Ultralong Fluorescence Lifetimes in a Donor-Acceptor Emitter Featuring a Hybrid Sulfone-Triarylboron Acceptor**. *Angew. Chemie - Int. Ed.* **2023**, *62*.

(11) Serevičius, T.; Skaisgiris, R.; Dodonova, J.; Kazlauskas, K.; Juršėnas, S.; Tumkevičius, S. Minimization of Solid-State Conformational Disorder in Donor–Acceptor TADF Compounds. *Phys. Chem. Chem. Phys.* **2020**, *22*, 265–272.

(12) Nasu, K.; Nakagawa, T.; Nomura, H.; Lin, C.-J.; Cheng, C.-H.; Tseng, M.-R.; Yasuda, T.; Adachi, C. A Highly Luminescent Spiro-Anthracenone-Based Organic Light-Emitting Diode Exhibiting Thermally Activated Delayed Fluorescence. *Chem. Commun.* **2013**, *49*, 10385.

(13) Okamura, N.; Maeda, T.; Fujiwara, H.; Soman, A.; Unni, K. N. N.; Ajayaghosh, A.; Yagi, S. Photokinetic Study on Remarkable Excimer Phosphorescence from Heteroleptic Cyclometalated Platinum(<scp>ii</Scp>) Complexes Bearing a Benzoylated 2-Phenylpyridinate Ligand. *Phys. Chem. Chem. Phys.* **2018**, *20*, 542–552.

(14) Murphy, L.; Brulatti, P.; Fattori, V.; Cocchi, M.; Williams, J. A. G. Blue-Shifting the Monomer and Excimer Phosphorescence of Tridentate Cyclometallated Platinum(Ii) Complexes for Optimal White-Light OLEDs. *Chem. Commun.* **2012**, *48*, 5817.

(15) Salthouse, R. J.; Pander, P.; Yufit, D. S.; Dias, F. B.; Williams, J. A. G. Near-Infrared Electroluminescence beyond 940 Nm in Pt(N^C^N)X Complexes: Influencing Aggregation with the Ancillary Ligand X. *Chem. Sci.* **2022**, *13*, 13600–13610.

(16) Shafikov, M. Z.; Pander, P.; Zaytsev, A. V.; Daniels, R.; Martinscroft, R.; Dias, F. B.; Williams, J. A. G.; Kozhevnikov, V. N. Extended Ligand Conjugation and Dinuclearity as a Route to Efficient Platinum-Based near-Infrared (NIR) Triplet Emitters and Solution-Processed NIR-OLEDs. *J. Mater. Chem. C* **2021**, *9*, 127–135.

(17) Pander, P.; Daniels, R.; Zaytsev, A. V.; Horn, A.; Sil, A.; Penfold, T. J.; Williams, J. A. G.; Kozhevnikov, V. N.; Dias, F. B. Exceptionally Fast Radiative Decay of a Dinuclear Platinum Complex through Thermally Activated Delayed Fluorescence. *Chem. Sci.* **2021**, *12*, 6172–6180.

(18) Wei, Y.-C.; Wang, S. F.; Hu, Y.; Liao, L.-S.; Chen, D.-G.; Chang, K.-H.; Wang, C.-W.; Liu, S.-H.; Chan, W.-H.; Liao, J.-L.; Hung, W.-Y.; Wang, T.-H.; Chen, P.-T.; Hsu, H.-F.; Chi, Y.; Chou, P.-T. Overcoming the Energy Gap Law in Near-Infrared OLEDs by Exciton–Vibration Decoupling. *Nat. Photonics* **2020**, *14*, 570–577.

(19) C, A.; Colella, M.; Griffin, J.; Kingsley, J.; Scarratt, N.; Luszczynska, B.; Ulanski, J. Slot-Die Coating of Double Polymer Layers for the Fabrication of Organic Light Emitting Diodes. *Micromachines* **2019**, *10*, 53.

(20) Fahlteich, J.; Steiner, C.; Top, M.; Wynands, D.; Wanski, T.; Mogck, S.; Kucukpinar, E.; Amberg-Schwab, S.; Boeffel, C.; Schiller, N. 10.1: Invited Paper : Roll-to-Roll Manufacturing of Functional Substrates and Encapsulation Films for Organic Electronics: Technologies and Challenges. *SID Symp. Dig. Tech. Pap.* **2015**, *46*, 106–110.

(21) Kamtekar, K. T.; Monkman, A. P.; Bryce, M. R. Recent Advances in White Organic Light-Emitting Materials and Devices (WOLEDS). *Adv. Mater.* **2010**, *22*, 572–582.

(22) Hung, W.-Y.; Fang, G.-C.; Lin, S.-W.; Cheng, S.-H.; Wong, K.-T.; Kuo, T.-Y.; Chou, P.-T. The First Tandem, All-Exciplex-Based WOLED. *Sci. Rep.* **2015**, *4*, 5161.

(23) Pereira, D. D. S.; dos Santos, P. L.; Ward, J. S.; Data, P.; Okazaki, M.; Takeda, Y.; Minakata, S.; Bryce, M. R.; Monkman, A. P. An Optical and Electrical Study of Full Thermally Activated Delayed Fluorescent White Organic Light-Emitting Diodes. *Sci. Rep.* **2017**, *7*, 6234.

(24) Jou, J.-H.; Su, Y.-T.; Hsiao, M.-T.; Yu, H.-H.; He, Z.-K.; Fu, S.-C.; Chiang, C.-H.; Chen,

C.-T.; Chou, C.; Shyue, J.-J. Solution-Process-Feasible Deep-Red Phosphorescent Emitter. *J. Phys. Chem. C* **2016**, *120*, 18794–18802.

(25) Strickler, S. J.; Berg, R. A. Relationship between Absorption Intensity and Fluorescence Lifetime of Molecules. *J. Chem. Phys.* **1962**, *37*, 814–822.

(26) Pander, P.; Sil, A.; Salthouse, R. J.; Harris, C. W.; Walden, M. T.; Yufit, D. S.; Williams, J. A. G.; Dias, F. B. Excimer or Aggregate? Near Infrared Electro- and Photoluminescence from Multimolecular Excited States of N^C^N-Coordinated Platinum(II) Complexes. *J. Mater. Chem. C* **2022**, *10*, 15084–15095.

(27) Rossi, E.; Colombo, A.; Dragonetti, C.; Roberto, D.; Ugo, R.; Valore, A.; Falciola, L.; Brulatti, P.; Cocchi, M.; Williams, J. A. G. Novel N^C^N-Cyclometallated Platinum Complexes with Acetylide Co-Ligands as Efficient Phosphors for OLEDs. *J. Mater. Chem.* **2012**, *22*, 10650–10655.

(28) Rossi, E.; Colombo, A.; Dragonetti, C.; Roberto, D.; Demartin, F.; Cocchi, M.; Brulatti, P.; Fattori, V.; Williams, J. A. G. From Red to near Infra-Red OLEDs: The Remarkable Effect of Changing from X = -Cl to -NCS in a Cyclometallated [Pt(N∧C∧N)X] Complex (N∧C∧N = 5-Mesityl-1,3-Di-(2-Pyridyl)Benzene). *Chem. Commun.* **2012**, *48*, 3182–3184.

(29) Cho, Y. J.; Kim, S. Y.; Son, H. J.; Cho, D. W.; Kang, S. O. Steric Effect on Excimer Formation in Planar Pt(II) Complexes. *Phys. Chem. Chem. Phys.* **2017**, *19*, 5486–5494.

(30) Pander, P.; Zaytsev, A. V.; Sil, A.; Williams, J. A. G.; Lanoe, P.-H.; Kozhevnikov, V. N.; Dias, F. B. The Role of Dinuclearity in Promoting Thermally Activated Delayed Fluorescence (TADF) in Cyclometallated, N^C^N-Coordinated Platinum(II) Complexes. *J. Mater. Chem. C* **2021**, *9*, 10276–10287.

(31) Walden, M. T.; Pander, P.; Yufit, D. S.; Dias, F. B.; Williams, G. J. A. Homoleptic Platinum(Ii) Complexes with Pyridyltriazole Ligands: Excimer-Forming Phosphorescent Emitters for Solution-Processed OLEDs. *J. Mater. Chem. C* **2019**, *7*, 6592–6606.

(32) Neese, F. Software Update: The <scp>ORCA</Scp> Program System—Version 5.0. *WIREs Comput. Mol. Sci.* **2022**, *12*.

(33) Becke, A. D. Density-functional Thermochemistry. III. The Role of Exact Exchange. *J. Chem. Phys.* **1993**, *98*, 5648–5652.

(34) Stephens, P. J.; Devlin, F. J.; Chabalowski, C. F.; Frisch, M. J. Ab Initio Calculation of Vibrational Absorption and Circular Dichroism Spectra Using Density Functional Force Fields. *J. Phys. Chem.* **1994**, *98*, 11623–11627.

(35) Weigend, F.; Ahlrichs, R. Balanced Basis Sets of Split Valence, Triple Zeta Valence and Quadruple Zeta Valence Quality for H to Rn: Design and Assessment of Accuracy. *Phys. Chem. Chem. Phys.* **2005**, *7*, 3297.

(36) Roemelt, M.; Maganas, D.; DeBeer, S.; Neese, F. A Combined DFT and Restricted Open-Shell Configuration Interaction Method Including Spin-Orbit Coupling: Application to Transition Metal L-Edge X-Ray Absorption Spectroscopy. *J. Chem. Phys.* **2013**, *138*, 204101.

(37) de Souza, B.; Farias, G.; Neese, F.; Izsák, R. Predicting Phosphorescence Rates of Light Organic Molecules Using Time-Dependent Density Functional Theory and the Path Integral Approach to Dynamics. *J. Chem. Theory Comput.* **2019**, *15*, 1896–1904.

(38) Lenthe, E. van; Baerends, E. J.; Snijders, J. G. Relativistic Regular Two-component Hamiltonians. *J. Chem. Phys.* **1993**, *99*, 4597–4610.

(39) van Lenthe, E.; Baerends, E. J.; Snijders, J. G. Relativistic Total Energy Using Regular Approximations. *J. Chem. Phys.* **1994**, *101*, 9783–9792.

(40) Pander, P.; Turnbull, G.; Zaytsev, A. V.; Dias, F. B.; Kozhevnikov, V. N. Benzannulation via the Use of 1,2,4-Triazines Extends Aromatic System of Cyclometallated Pt(II) Complexes to Achieve Candle Light Electroluminescence. *Dye. Pigment.* **2021**, *184*,

108857.

(41) Yersin, H.; Rausch, A. F.; Czerwieniec, R.; Hofbeck, T.; Fischer, T. The Triplet State of Organo-Transition Metal Compounds. Triplet Harvesting and Singlet Harvesting for Efficient OLEDs. *Coordination Chemistry Reviews*. Elsevier B.V. 2011, pp 2622–2652.

(42) Baryshnikov, G.; Minaev, B.; Ågren, H. Theory and Calculation of the Phosphorescence Phenomenon. *Chem. Rev.* **2017**, *117*, 6500–6537.

(43) Pashazadeh, R.; Pander, P.; Lazauskas, A.; Dias, F. B.; Grazulevicius, J. V. Multicolor Luminescence Switching and Controllable Thermally Activated Delayed Fluorescence Turn on/Turn off in Carbazole-Quinoxaline-Carbazole Triads. *J. Phys. Chem. Lett.* **2018**, *9*, 1172–1177.

(44) Urban, M.; Marek-Urban, P. H.; Durka, K.; Luliński, S.; Pander, P.; Monkman, A. P. TADF Invariant of Host Polarity and Ultralong Fluorescence Lifetimes in a Donor-Acceptor Emitter Featuring a Hybrid Sulfone-Triarylboron Acceptor**. *Angew. Chemie Int. Ed.* **2023**, *62*.

(45) Vasylieva, M.; Pander, P.; Sharma, B. K.; Shaikh, A. M.; Kamble, R. M.; Dias, F. B.; Czichy, M.; Data, P. Acridone-Amine D-A-D Thermally Activated Delayed Fluorescence Emitters with Narrow Resolved Electroluminescence and Their Electrochromic Properties. *Electrochim. Acta* **2021**, *384*, 138347.

(46) Kourkoulos, D.; Karakus, C.; Hertel, D.; Alle, R.; Schmeding, S.; Hummel, J.; Risch, N.; Holder, E.; Meerholz, K. Photophysical Properties and OLED Performance of Light-Emitting Platinum(Ii) Complexes. *Dalt. Trans.* **2013**, *42*, 13612.

Table of Contents

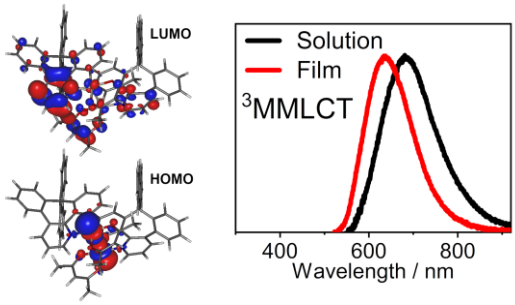

A novel, highly soluble platinum(II) complex displays unusual behaviour of the excimer/dimer ^{3}MMLCT emission in solid films.